

Figure S1. Generation of TERT-ER knock-in chimeras and validation of germline transmission. (a) Schematic of targeting vector used to generate the knock-in mTERT-ER allele. TG: targeting vector; WT, wild type allele; KI, knock-in allele; SfiI, enzyme used to linearize the vector; LA, left arm; KF, Kozak-Flag sequence; ER, modified estrogen receptor (ERT2) ligand binding domain; I, II, exons I and II; black triangles, loxP sequences; pgk-neo, pgk promoter and G418 resistance gene; RA, Right arm; DT, diphtheria toxin gene; BamHI, enzyme used for the screening. All TERT-ER mice used in this study derive from TERT-ERneo x EIIA-cre crosses. Of note, the EIIA-cre allele was bred out to eliminate unspecific DNA damage caused by persistent CRE recombinase activity (b) Southern blot probed with 3' probe showing germline transmission of mTERT-ERneo allele in pups 1 and 3. M, molecular weight markers (c) Genotyping primers distinguish between wt TERT, TERT-ERneo and TERT-ER alleles after CRE deletion. Representative gel showing PCR products derived from genomic DNA from several tissues harvested from a heterozygous (G0) and a homozygous (G4) TERT-ER mouse. (d, e) Expression levels for wildtype TERT (white) and TERT-ER (black) alleles by quantitative real-time PCR in various tissues harvested from a heterozygous (G0) TERT-ER mouse relative to housekeeping gene R15 (d) and each other (e).

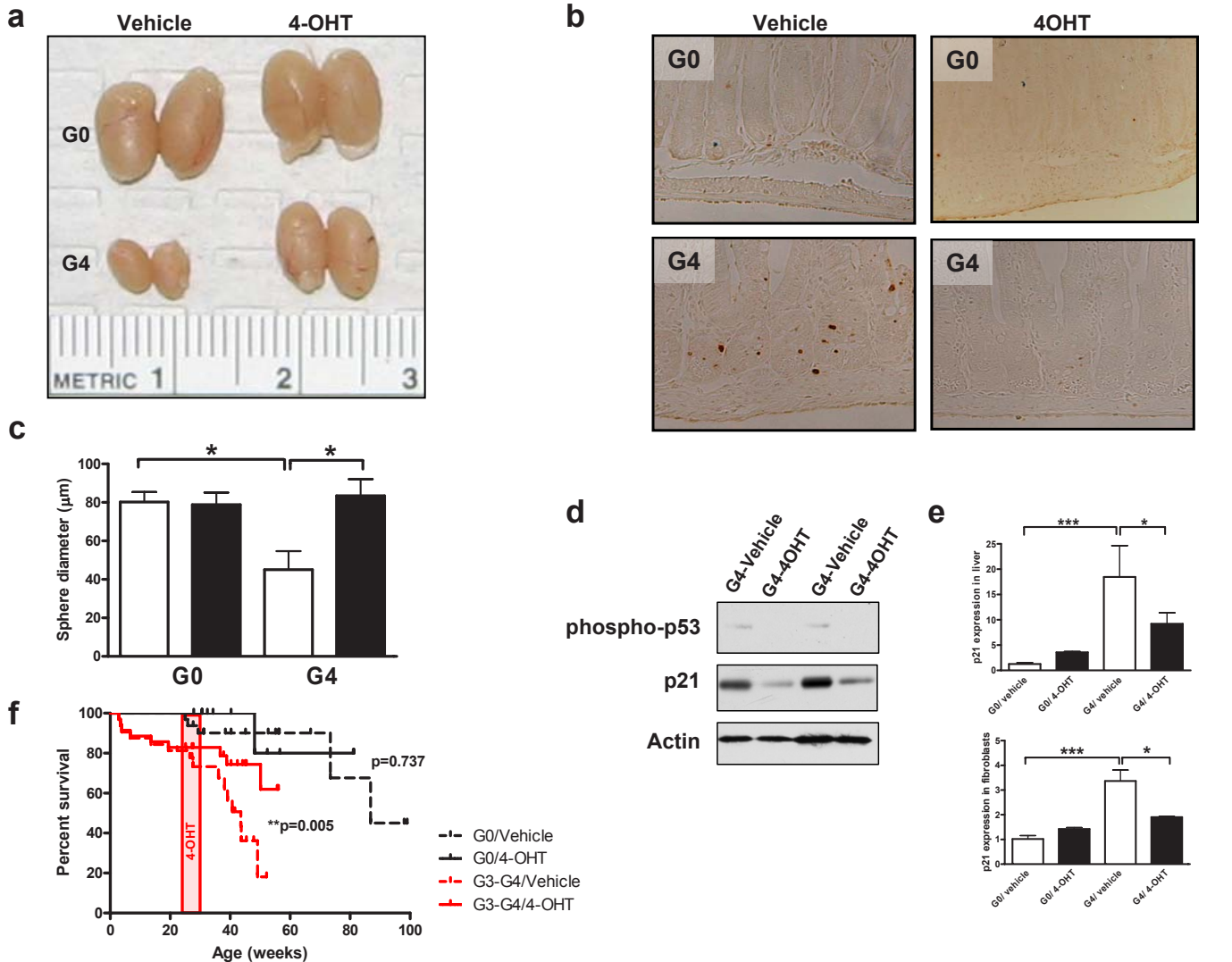


Figure S2. Effects of telomerase reactivation on adult TERT-ER testes, intestinal crypts, liver, NSCs and overall survival. (a) Representative photograph of testes from age-matched G0 (top) and G4 (bottom) TERT-ER mice, treated for 4 weeks with vehicle (left) or 4-OHT (right). (b) Small intestine sections from age-matched G0 (top) and G4 (bottom) TERT-ER mice, treated for 4 weeks with vehicle (left) or 4-OHT (right) were stained with a TUNEL kit to visualize apoptotic cells. (c) Average neurosphere size (long axis) for G0 and G4^{TERT-ER} NSCs cultured for 2 weeks in the presence of vehicle (open bars) or 100nM 4-OHT (filled bars). (d) Western blot of liver protein extracts probed with antibodies specific for phospho-p53 (Ser15), p21 and β -actin. (e) p21 expression in liver and in adult skin fibroblasts as determined by RT-PCR. (f) Kaplan-Meier analysis of overall survival for G0 (black) and G4^{TERT-ER} (red) males. The pink rectangle represents the window of treatment with 4-OHT (solid line) or vehicle (dotted line). G0/vehicle, n=32; G0/4-OHT, n=21; G4/vehicle, n=32; G4/4-OHT, n=29.

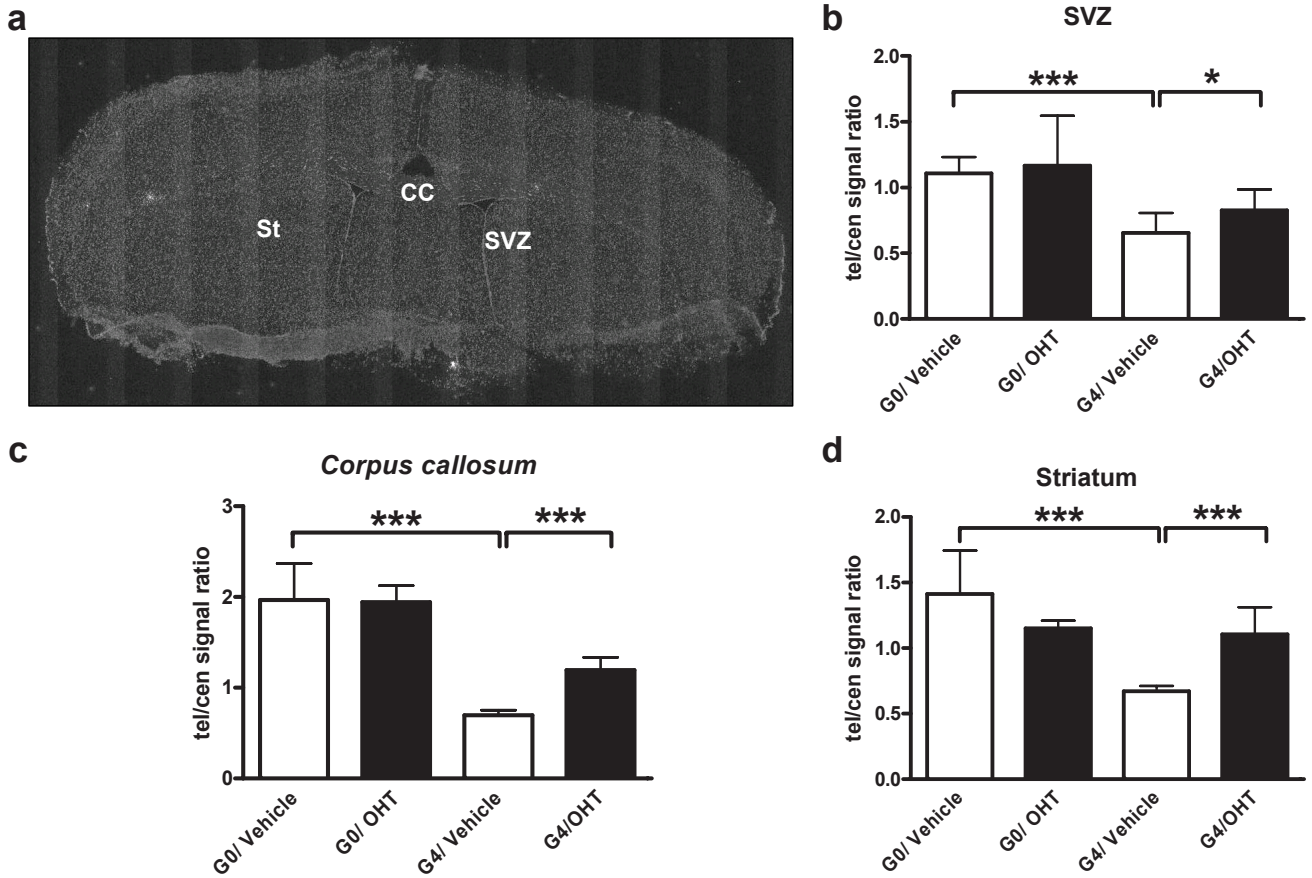


Figure S3. Telomere elongation after telomerase reactivation in the brain. (a) Representative scanning of a brain frozen section stained for nucleus visualization showing the selected areas for quantitative FISH analysis. SVZ, subventricular zone; CC, *corpus callosum*; St: *striatum*. (b,c,d) Telomeric-specific FISH signal relative to centromeric signal is depicted for SVZ, CC and striatum (St). Genotypes and treatment regimens are indicated along the x axis for each sample.

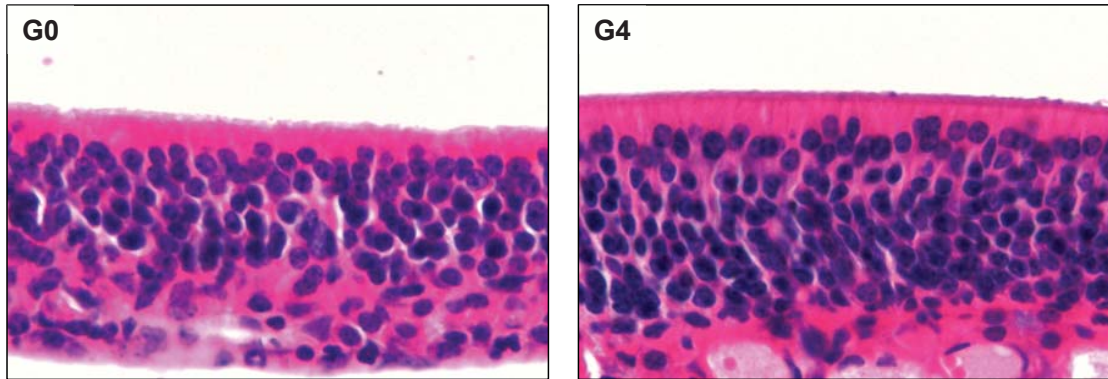


Figure S4. Olfactory epithelium is not grossly affected by telomere dysfunction.
Representative H&E stained section of olfactory epithelium from the olfactory turbinate of an adult G0 (left) and a G4 (right) TERT-ER mouse.

[2-MB] (M)	G0 TERT-ER	G4 TERT-ER
0	819	689
1.7×10^{-6}	486	422
1.7×10^{-5}	545	400
1.7×10^{-4}	431	487

Table S1. Mean total distance moved (cm) during testing period ($p > 0.05$)

[2-MB] (M)	G0/placebo	G4/placebo	G0/4OHT	G4/4OHT
0	7	11	6	6
1.7×10^{-6}	2	4	2	2
1.7×10^{-5}	1	6 ^{***}	1	1
1.7×10^{-4}	1	1	1	2

Table S2. Mean frequency of entry into odor zone (n) ($p < 0.0001$).**

	Forward	Reverse
<i>p21</i>	AGCCTGAAGACTGTGATGGG	AAAGTTCCACCGTTCTCGG
<i>gapdh</i>	GACCCCTTCATTGACCTCAACT AC	TGGTGGTGCAGGATGCATTGC TGA
<i>wt- tert</i>	TGGGGCCCGAGGGCAGGCCGG	GCTCGCAGAGTCTCTGCACA
<i>tert-ER</i>	ATGACCTGCTGCTGGAGATG	AAAGGTTGCCAGCGGCCACA

Table S3. Oligonucleotide primer sequences used for RT-PCR.